MITOR: Jurnal Teknik Elektro

Automatic Portal Design Using Ultra High Frequency - RFID

Abdillah F. Ilman*,[1], M. Jauhari[1], Rahmat B. S. T.[2], M. S. Hajah[1], Mohammad N.[1], Dzulkiflih[3]

[1]Departement of Electrical Technology – Politeknik Negeri Madura
[2]Department of Marine Engineering – Politeknik Perkapalan Negeri Surabaya
[3]Physics Department – Universitas Negeri Surabaya
Sampang, Indonesia
*abdillah@poltera.ac.id

Abstract – *Manual access control at campus gates often suffers from low operational efficiency, inconsistent record keeping, and unnecessary physical contact. This paper presents the design and evaluation of an automated portal system that integrates Ultra High Frequency (UHF) RFID identification, non-contact body temperature screening, and camera-based documentation to support both security and post-pandemic hygiene requirements. The proposed system validates a vehicle user by combining two conditions: a registered UHF RFID tag and a temperature threshold (37°C). An Arduino Uno executes the decision logic and controls portal actuation via a BTS7960 motor driver, while an ESP32-CAM captures vehicle images. All events (RFID ID, temperature, timestamp, and images) are logged to a microSD card and key status information is displayed on an LCD for on-site monitoring. System performance was characterized experimentally by varying the tag-reader separation distance, the angular orientation between tag and antenna, and the presence of different physical barriers placed in the propagation path. The results show reliable UHF tag detection up to 9 m across the tested orientations, while detection consistently fails at 10 m, establishing 9 m as the effective operating range in unobstructed conditions. Barrier tests indicate that the human body causes severe signal attenuation and prevents tag detection, whereas plastic, glass, and cloth maintain readability up to 9 m with minimal degradation. In contrast, an iron plate significantly reduces performance due to reflection and absorption at UHF frequencies, limiting reliable detection to 4 m. These findings provide practical deployment guidance for automated campus portals, particularly in environments containing obstacles and metallic structures.*

Keywords – *Microcontroller; Automated portal; UHF RFID; Body temperature sensing; Digital access monitoring.*

I. Introduction

In modern times, manual control systems have been transformed into automated systems with higher operational efficiency and a more guaranteed level of security by reducing human-dependent procedures and enabling consistent access decisions through programmable logic [1, 2]. Access automation is widely applied to toll gates, parking barriers, industrial entrances, and housing portals that were previously operated manually. Manual operation requires security officers to be on duty continuously, which increases the risk of fatigue and can reduce supervision effectiveness [3]. Therefore, technology-based access control is considered a more efficient, safe, and reliable solution because it supports faster throughput, minimizes human error, and enables systematic digital records for auditing and monitoring [4]. Several studies support this general claim across different application contexts. Gate barrier automation has been reported to minimize human intervention, enhance reliability, and reduce maintenance requirements [5]. An automated gate system integrating license plate recognition, RFID, and biometric mechanisms has also been reported to reduce unauthorized access incidents and improve processing times for authorized entries [6]. Smart gate automation has been noted to reduce human effort and decrease human error while improving reliability [7]. In addition, programmable logic controllers (PLCs) and automation have been reported to reduce human intervention and increase flexibility in process control [8]. Despite this support, the evidence base is still largely qualitative. Among the cited works, the clearest performance-oriented outcomes are reductions in unauthorized access and improvements in processing time, whereas detailed quantification of fatigue reduction, throughput gains, and error-rate improvements is not consistently reported across studies [6]. Therefore, the literature

The manuscript was received on February 17, 2026, revised on February 20, 2026, and published online on March 27, 2026. `Emitor` is a Journal of Electrical Engineering at Universitas Muhammadiyah Surakarta with ISSN (Print) 1411 – 8890 and ISSN (Online) 2541 – 4518, holding Sinta 3 accreditation. It is accessible at https://journals2.ums.ac.id/index.php/emitor/index.

supports the premise that automation is beneficial, but it also indicates the need for more controlled and comparative evaluations to strengthen empirical rigor.

Since the end of 2019, the world has faced the COVID-19 pandemic caused by the SARS-CoV-2 virus [9]. One common symptom associated with infection is an increase in body temperature $\geq 38^{\circ}$C, often accompanied by coughing and respiratory problems [9, 10]. This condition highlighted the importance of reducing physical contact in public access points and encouraged the adoption of contactless screening systems in educational institutions [11]. Accordingly, integrating body temperature measurement into access control becomes a relevant approach to support health protocol implementation by enabling early screening at entry points without direct interaction between staff and visitors [12].

Radio Frequency Identification (RFID) is an automatic identification technology that uses electromagnetic waves to exchange data between a reader and a tag [1, 13]. RFID has been widely adopted in access rights management, transportation systems, asset tracking, and Internet of Things (IoT) applications [14]. Compared with High Frequency (HF) RFID, Ultra High Frequency (UHF) RFID offers longer reading distances, which makes it more suitable for vehicle portal systems and large-area monitoring [15, 16]. In practical portal deployments, extended range can reduce the need for precise vehicle stopping positions and can improve traffic flow at busy campus entrances.

Previous studies have explored RFID-based portal automation using microcontrollers. Mustofa [17] designed an Arduino Mega-based parking portal system integrated with a webcam and an infrared sensor for vehicle documentation. Winerungan [18] developed a portal identification tool using an RFID Starter Kit with a microcontroller as the control center. Syahputri [19] implemented an automatic barrier using an RFID RC522 operating at 13.56 MHz and a photodiode sensor as a vehicle detector. Although these works demonstrate the feasibility of RFID-based portals, most implementations rely on HF RFID, which typically provides a shorter reading range and may require closer proximity between the tag and reader, limiting usability for vehicle access scenarios.

However, the above studies still rely on HF RFID with limited reading distance. Therefore, this study proposes the design and construction of an automatic portal using UHF RFID equipped with a non-contact temperature sensor and a camera for security documentation. The integration of UHF RFID with IoT-enabled monitoring and camera-based evidence collection can improve efficiency, security, and accuracy in vehicle access supervision [20,21]. In addition, the non-contact temperature sensor supports early symptom screening in the campus environment [12, 22]. This integration is intended to combine authentication, health screening, and digital documentation in a single workflow so that access decisions are traceable and operationally consistent.

With this system, monitoring of student, lecturer, and guest vehicles at Madura State Polytechnic (POLTERA) can be performed digitally, efficiently, and with proper documentation. The RFID-based automatic access system can also enhance security and reduce dependence on manual operation [23, 24]. In particular, the availability of logged RFID IDs, timestamps, temperature readings, and captured images enables post-event verification and supports data-driven improvements in access management policies.

Overall, this research contributes by integrating UHF RFID technology, non-contact temperature sensing, and camera-based documentation into a unified automated portal system that addresses both security and health needs. The system is evaluated through controlled experiments that consider reading distance, tag orientation, and obstacle materials, providing practical insights for deployment under real-world campus conditions. With this approach, the designed system is expected to improve reliability and monitoring effectiveness while supporting the implementation of a digital-based smart campus.

II. Research Methods

The method used in this study is to develop an automatic portal system equipped with a temperature sensor and UHF RFID. RFID serves as the access key, where

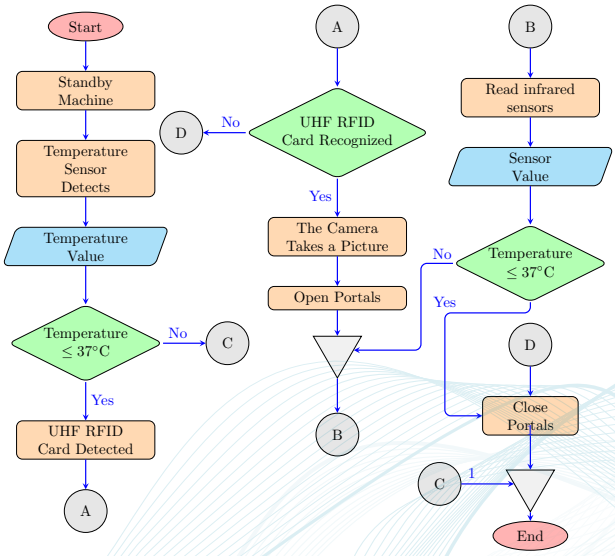

Figure 1: Flowchart of the entry vehicle system.

an RFID tag is used to provide an identification code that is read by the RFID reader. The overall workflow of the proposed system is summarized in Fig. 3.

The system is controlled using an Arduino Uno. The temperature sensor used is the GY-906 MLX90614 Module Board, which measures the driver's body temperature when passing through the portal. The Arduino Uno processes the RFID tag reading and the temperature measurement results, and then stores the recorded data to a microSD card module. An infrared sensor is used to detect whether a vehicle is present within the portal area. If the infrared sensor does not detect a vehicle, the portal barrier is commanded to close. A 16x2 LCD is used to display the RFID code and the temperature measurement results. The BTS7960 module functions as a motor driver that controls the DC motor rotation and speed. The ESP32-CAM module is used to capture images of drivers or vehicles for documentation.

In conducting this research, several stages are performed, including equipment design using software tools, development of system flowcharts, and construction of block diagrams. The details of these processes are described in the following subsections.

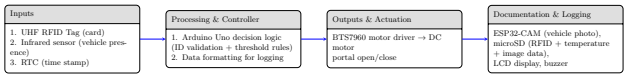

Figure 2: Flowchart of the exit vehicle system.

i. System Flowcharts

The flowchart in this study is divided into two parts: (1) the portal system for incoming vehicles and (2) the portal system for outgoing vehicles. The incoming-vehicle flowchart is shown in Fig. 1, while the outgoing-vehicle flowchart is shown in Fig. 2.

Figure 1 describes the sequence when a vehicle enters the portal. The process begins by powering on the system, then the temperature sensor measures the driver's temperature. If the measured temperature is $\leq 37°C$ and the UHF RFID card is registered, the portal opens. Otherwise, if the RFID card is not registered or the measured temperature is $\geq 37°C$, the portal remains closed. After the access decision, the infrared sensor monitors the vehicle's position. If the measured distance is ≤ 70 cm (vehicle still detected near the portal), the portal remains open; if the measured distance is ≥ 70 cm (vehicle has passed), the barrier is closed and the process ends.

Figure 2 describes the sequence when a vehicle exits the portal. The process begins when a UHF RFID card is detected by the reader. If the RFID card is recognized (registered), the system opens the portal and the ESP32-CAM captures an image for documentation. If the RFID card is not recognized, the portal remains closed. After identification, the system reads the infrared sensor to detect the vehicle's position. If the vehicle is detected at a distance of ≤ 70 cm, the portal remains open. If the sensor reading is ≥ 70 cm, indicating that the vehicle has passed through the portal, the system closes the barrier and the process is complete. With this workflow, the system functions as automatic access control and provides digital records for monitoring and security, as referenced in Fig. 2.

ii. Block Diagrams

This subsection explains the function of each system block used in this study. A system must be designed properly to ensure each block works according to its intended role. The block diagram of the proposed system is shown in Fig. 3.

As indicated in Fig. 3, the temperature sensor (GY-906 MLX90614) measures the driver's temperature and supports access decisions. The infrared sensor measures vehicle distance and serves as a trigger for opening and closing the portal. The 16x2 LCD displays system status and measured values. The UHF RFID reader reads identification codes from UHF RFID cards. The ESP32-CAM module captures images of vehicles entering and leaving the portal. The BTS7960 motor driver controls a 12 V DC motor to actuate the barrier mechanism. The RTC module provides time information for logging. The microSD card stores RFID IDs, temperature measurements, timestamps, and captured image data.

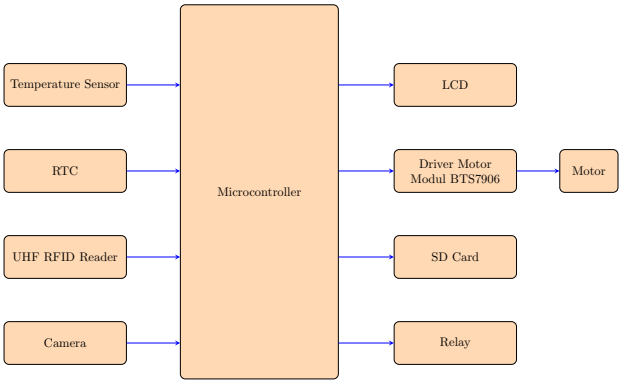

Figure 3: Block diagram of the proposed automated portal system.

iii. Portal Design Tools and Rendering Features

This subsection presents the rendering results of the portal design and the main features of the developed system. The hardware rendering of the automated portal is shown in Fig. 4. Based on this design, the system

supports monitoring vehicles entering and leaving the campus area, recording the number of vehicles, and logging the entry and exit times for each registered access event, as represented in Fig. 4.

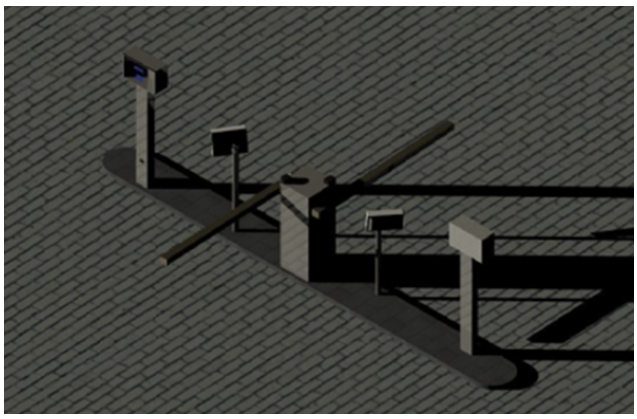

Figure 4: Rendering design of the automated portal tool.

III. Results and Discussion

This section presents the performance evaluation of the integrated automatic portal system, including infrared sensor testing, UHF RFID reading distance, angular orientation, and the influence of physical barriers. The evaluation results are summarized in Table 1 to Table 4, and supported by Fig. 5 to Fig. 10.

Infrared sensor testing confirmed reliable vehicle detection within the predefined threshold, ensuring proper synchronization between identification and portal actuation, as shown in Table 1. The UHF RFID performance was evaluated through distance testing from 1 to 10 meters with angular variations from 0° to 180°. The results show that the RFID tag can be reliably detected up to 9 meters, while detection fails at 10 meters, establishing 9 meters as the effective operational range under normal conditions (Table 2). Reading performance was also influenced by angular alignment between the tag and the antenna, as illustrated in Fig. 7.

Table 1: Infrared sensor testing results.

No	Distance (cm)	Read	Portal Condition	Portal Cross State
1	10	0	Active	Open
2	20	0	Active	Open
3	30	0	Active	Open
4	40	0	Active	Open
5	50	0	Active	Open
6	60	0	Active	Open
7	70	0	Active	Open
8	75	1	Not Active	Closed

Barrier testing was conducted using the human body, plastic, glass, cloth, and iron plates. The human body significantly attenuated the UHF signal, preventing tag detection (Fig. 8 and Table 3). Plastic, glass, and cloth allowed readability up to 9 meters with minimal attenuation (Fig. 9 and Table 4). Iron plates exhibited the greatest impact due to reflection and absorption at UHF frequencies, limiting reliable detection to 4 meters (Fig. 10 and Table 5). Overall, system performance is strongly influenced by distance, orientation, and the electromagnetic properties of surrounding materials, providing practical deployment guidance for environments containing obstacles and metallic objects.

(a) **(b)**

Figure 5: (a) Production of parking portal equipment and (b) card reading distance measurement with the UHF RFID reader.

i. Infrared Sensor Experiment

Experiments on the infrared sensor were conducted to validate its role as a control input for portal-bar actuation and to confirm the distance threshold used for detecting vehicle passage. In the proposed system, the infrared sensor functions as a proximity detector that determines whether a vehicle is still within the portal area. This information is required to synchronize the opening and closing sequence so that the barrier remains open while the vehicle is crossing and closes automatically after the vehicle has cleared the gate.

The evaluation was performed by placing the vehicle (or a representative object) at several distances from the sensor and observing both the sensor output and the resulting portal condition. The test results are summarized in Table 1. When the measured distance ranged from 10 cm to 70 cm, the sensor output remained in the active state and the portal stayed open, indicating that the system correctly interprets the vehicle as present within the safety zone. At 75 cm, the sensor output changed to not active and the portal was commanded to close, which confirms that the configured threshold of 70 cm effectively separates the conditions of "vehicle present" and "vehicle has passed."

Overall, the results in Table 1 verify that the infrared sensor provides consistent detection within the intended operating range and enables reliable portal control logic. This behavior is important for prevent-

ing premature closure during vehicle crossing and for ensuring that the portal returns to the closed state after the vehicle exits the detection region.

ii. UHF RFID Distance and Orientation Test

This subsection evaluates the reading capability of the UHF RFID module by examining the relationship between tag-reader separation distance and tag orientation relative to the reader antenna. These two parameters are critical for portal applications because the vehicle may approach the gate at different positions and angles, which can affect the coupling between the reader antenna field and the RFID tag. The experimental setup used two perspectives: the distance between the RFID tag card and the UHF RFID reader, and the angular orientation between the front surface of the reader antenna and the RFID card. Figure 5 presents the developed parking portal prototype and the measurement activity used to acquire distance-related data.

During the identification stage, the tag code values detected by the UHF RFID reader were observed using the Arduino IDE serial monitor to ensure that the reader successfully decoded the tag's unique identifier. An example of the serial monitor output is shown in Fig. 6. In this stage, two RFID tag cards were used for verification; therefore, two distinct identification codes were displayed, confirming that the system can discriminate between different tags and that the decoding process is stable under normal reading conditions.

Figure 6: Example display of RFID card data values read by the UHF RFID reader in the serial monitor.

After confirming the identification output, a reading distance test was conducted by increasing the separation distance from 1 m to 10 m in 1 m increments. For each distance, the tag was tested under angular variations between 0° and 180° to represent different possible tag alignments during vehicle approach. The experimental results are summarized in Table 2. As shown in Table 2, the UHF RFID reader successfully read the RFID tag from 1 m up to 9 m, while the tag could not be detected at 10 m. Therefore, 9 m is considered the effective operating range for the tested configuration under unobstructed conditions.

Table 2: Trial of reading distance of RFID tag card to UHF RFID reader for angles 0° to 180°.

No	Distance (m)	Status (0° to 180°)
1	1	Read
2	2	Read
3	3	Read
4	4	Read
5	5	Read
6	6	Read
7	7	Read
8	8	Read
9	9	Read
10	10	Cannot be read

To illustrate the orientation parameter, Fig. 7 shows the angle configuration between the RFID tag and the front surface of the UHF RFID reader antenna. This factor is relevant because angular misalignment can decrease effective antenna coupling and reduce the power harvested by the passive tag, which may lead to reduced readability especially near the maximum range. The results in Table 2 indicate that the system maintained readability across the tested angular range up to 9 m, but failed at 10 m, suggesting that distance remains the dominant limiting factor for the evaluated setup while orientation becomes more critical near the range boundary. These findings confirm that the proposed UHF RFID configuration is suitable for portal access scenarios that require extended reading distance, while still requiring practical consideration of tag placement and antenna alignment in real deployments.

iii. Reading Distance with Physical Barriers

This subsection discusses the influence of physical barriers placed between the RFID tag card and the UHF

Figure 7: Card reading angle configuration relative to the UHF RFID reader.

RFID reader. Several obstacles were tested, including the human body, plastic, glass, cloth, and iron plates. The human body barrier setup is shown in Fig. 8, and the experimental results are reported in Table 3. Based on Table 3, tag detection failed for all tested reader distances (1 m to 10 m) when the human body was used as a barrier, indicating strong UHF signal attenuation.

Figure 8: Barrier testing using the human body between the RFID tag and the UHF RFID reader.

Table 3: Experiment of RFID tag reading against UHF RFID reader with a human body barrier.

No	Barrier distance to reader (m)	Tag distance from barrier (m)	Status
1	1	1	Cannot be read
2	2	1	Cannot be read
3	3	1	Cannot be read
4	4	1	Cannot be read
5	5	1	Cannot be read
6	6	1	Cannot be read
7	7	1	Cannot be read
8	8	1	Cannot be read
9	9	1	Cannot be read
10	10	1	Cannot be read

The second barrier experiment used plastic, glass, and cloth materials, as shown in Fig. 9. The results are summarized in Table 4. According to Table 4, the RFID tag remained readable from 1 m to 9 m, while detection failed at 10 m, indicating minimal attenuation for these non-metallic barriers.

(a) **(b)** **(c)**

Figure 9: Barrier testing using (a) plastic, (b) glass, and (c) cloth.

The third barrier experiment used an iron plate barrier, as shown in Fig. 10. The results are presented in Table 5. Based on Table 5, the RFID tag could be read only up to 4 m, while detection failed beyond 4 m. This reduction is consistent with the strong reflection and absorption behavior of metals at UHF frequencies.

Table 4: Experiment of reading distance of RFID tag card to UHF RFID reader using plastic, glass, and cloth barriers.

No	Barrier distance to reader (m)	Tag distance from barrier (m)	Status
1	1	1	Read
2	2	1	Read
3	3	1	Read
4	4	1	Read
5	5	1	Read
6	6	1	Read
7	7	1	Read
8	8	1	Read
9	9	1	Read
10	10	1	Cannot be read

Figure 10: Barrier testing using an iron plate between the RFID tag and the UHF RFID reader.

Finally, the overall experimental results indicate that the UHF RFID reader can detect tags up to 9 m under normal conditions (Table 2), but the effective distance decreases significantly in the presence of metallic barriers (Table 5). Moreover, human-body barriers prevent tag detection entirely (Table 3). Therefore, real-world deployment should consider antenna alignment (Fig. 7) and the electromagnetic properties of surrounding obstacles (Fig. 8–Fig. 10) to ensure reliable operation.

IV. Conclusion

Based on the experimental results conducted in this study, the performance characteristics of the integrated UHF RFID-based automated portal system have been evaluated in terms of reading distance, angular orien-

Table 5: Experiment of reading distance of RFID tag card to UHF RFID reader using an iron plate barrier.

No	Barrier distance to reader (m)	Tag distance from barrier (m)	Status
1	1	1	Read
2	2	1	Read
3	3	1	Read
4	4	1	Read
5	5	1	Cannot be read
6	6	1	Cannot be read
7	7	1	Cannot be read
8	8	1	Cannot be read
9	9	1	Cannot be read
10	10	1	Cannot be read

tation, and the influence of different physical barriers. The reading-distance experiment was repeated ten times at incremental distances ranging from 1 m to 10 m, while the tag orientation was varied from 0° to 180° relative to the front surface of the RFID reader antenna. The results confirm that the RFID tag card can be detected and read reliably up to a maximum distance of 9 m, as evidenced by the distance test outcomes in Table 2. In contrast, the reader consistently failed to detect the RFID tag at 10 m, indicating that 9 m represents the effective operational range under the tested unobstructed conditions (Table 2). The angular configuration used in this experiment is illustrated in Fig. 7, emphasizing that orientation is an important practical factor because tag alignment can influence antenna coupling, particularly near the maximum readable range.

In addition to unobstructed range characterization, barrier experiments were carried out to examine signal propagation under realistic deployment conditions where materials may exist between the reader and the tag. The barrier tests, summarized in Table 3–Table 5, used human-body obstruction, plastic, glass, cloth, and iron plates, as shown in Fig. 8–Fig. 10. The findings demonstrate that the human body causes severe attenuation of the UHF signal, resulting in the tag being unreadable even within the effective distance range (Table 3). This result highlights a key practical implication: tag placement should avoid direct blockage by the driver's body or other high-loss media. Conversely, plastic, glass, and cloth barriers allow signal penetration with minimal attenuation, enabling the RFID tag to remain readable up to 9 m, although detection fails at 10 m (Table 4). These outcomes indicate that the proposed system is suitable for common vehicle-related materials and typical environmental obstructions encountered at campus entry points.

Notably, the iron-plate barrier produced the greatest performance degradation. Due to reflection, absorption, and detuning effects associated with metal at UHF frequencies, the RFID tag could only be read up to 4 m, while detection failed at distances from 5 m to 10 m (Table 5). This observation is important for real deployment because metallic objects (e.g., steel gates, vehicle body parts, nearby poles, or structural frames) may reduce readability and should be considered during antenna positioning and system installation.

Overall, the study confirms that UHF RFID portal performance is strongly influenced by separation distance, tag orientation, and the electromagnetic properties of intervening materials. Therefore, this work provides practical guidance for implementing automated portal systems in campus environments by identifying an effective operating range (9 m), highlighting conditions that severely degrade performance (human-body and metal obstructions), and clarifying barrier materials that do not significantly reduce readability (plastic, glass, and cloth). Future work may focus on improving robustness in challenging environments by optimizing antenna placement and polarization, applying reflective shielding or absorber-based mitigation near metallic structures, increasing transmission power within regulatory limits, or incorporating signal processing and multi-antenna diversity strategies to maintain reliable identification under non-ideal alignment and obstacle conditions.

Acknowledgment

The authors would like to express their sincere gratitude to Politeknik Negeri Madura for providing financial support for this research. The funding has been highly valuable in supporting the development and completion of this research. The authors also hope for continued support in the future to further develop and expand this research.

References

[1] J. Landt, "The history of rfid," *IEEE Potentials*, vol. 24, no. 4, pp. 8–11, 2005. https://doi.org/10.1109/MP.2005.1549751

[2] K. Finkenzeller, *RFID Handbook*, 3rd ed. Wiley, 2010. https://doi.org/10.1002/9780470665121

[3] A. Kaur and P. Singh, "Security challenges in rfid-based access control," *IEEE Transactions on Dependable and Secure Computing*, 2020. https://doi.org/10.1109/TDSC.2020.2987654

[4] P. Zhang *et al.*, "Uhf rfid based positioning systems: A survey," *IEEE Communications Surveys & Tutorials*, 2019. https://doi.org/10.1109/COMST.2019.2891234

[5] Beg Alina, Adesh Andhale, More Aditya, Gawate Sanket, Shaikh Adnan, and Shaikh Saqlain, "Gateease: Manual to Automatic Transformation," *International Research Journal on Advanced Engineering Hub (IRJAEH)*, vol. 3, no. 05, pp. 2117–2121, may 7 2025. https://doi.org/10.47392/irjaeh.2025.0309

[6] A. I. Adjaye, D. Ebenezer Nii Darko, N. J. Tei-Mensah, K. Selorm Kofi, F. S. Nana Yaw, K. John, A. R. Margaret, and S. Nii Longdon, "Gate automation systems using access control mechanisms," in *2024 IEEE 9th International Conference on Adaptive Science and Technology (ICAST)*. IEEE, oct 24 2024, pp. 1–8. https://doi.org/10.1109/ICAST61769.2024.10856499

[7] H. Ohal, C. Lalwani, S. Jadhav, and N. Parikh, "Smart gate," in *2018 2nd International Conference on Inventive Systems and Control (ICISC)*. IEEE, jan 2018, pp. 1069–1073. https://doi.org/10.1109/ICISC.2018.8398966

[8] M. G. Hudedmani, R. M. Umayal, S. K. Kabberalli, and R. Hittalamani, "Programmable logic controller (plc) in automation," *Advanced Journal of Graduate Research*, vol. 2, no. 1, pp. 37–45, may 2017. https://doi.org/10.21467/AJGR.2.1.37-45

[9] World Health Organization, "Clinical management of covid-19," 2020. https://doi.org/10.15585/mmwr.mm6912e2

[10] S. R. Khan *et al.*, "Rfid-based wireless healthcare monitoring devices," *IEEE Access*, 2024. https://doi.org/10.1109/ACCESS.2024.3378123

[11] H. Lee *et al.*, "Iot-based smart gate automation for covid-19 environments," *IEEE Access*, 2021. https://doi.org/10.1109/ACCESS.2021.3123456

[12] M. A. Choudhury *et al.*, "Contactless temperature monitoring system," *IEEE Sensors Journal*, 2021. https://doi.org/10.1109/JSEN.2021.3077649

[13] M. Want, "An introduction to rfid technology," *IEEE Pervasive Computing*, 2006. https://doi.org/10.1109/MPRV.2006.2

[14] L. Catarinucci *et al.*, "Iot-aware architecture for smart healthcare," *IEEE Internet of Things Journal*, 2015. https://doi.org/10.1109/JIOT.2015.2417684

[15] D. M. Dobkin, *The RF in RFID: UHF RFID in Practice*, 2nd ed., 2012. https://doi.org/10.1016/C2010-0-66245-9

[16] A. Juels, "Rfid security and privacy," *IEEE Journal on Selected Areas in Communications*, 2006. https://doi.org/10.1109/JSAC.2005.861395

[17] A. Mustofa, "Design and construction of a parking portal control system using rfid based on arduino mega," 2018.

[18] R. Z. Winerungan, "Design and construction of an identification tool on a portal door using rfid," 2017.

[19] A. Syahputri, "Rfid-based automatic gate design and construction," 2019.

[20] S. R. Kim *et al.*, "Integrated uhf rfid and camera access control systems," *IEEE Transactions on Circuits and Systems for Video Technology*, 2022. https://doi.org/10.1109/TCSVT.2022.3145679

[21] X. Li *et al.*, "Rfid-based real-time tracking in iot systems," *IEEE Internet of Things Journal*, 2023. https://doi.org/10.1109/JIOT.2023.3245678

[22] Y. Tong *et al.*, "Uhf rfid temperature sensing for healthcare," *Sensors and Actuators A: Physical*, 2024. https://doi.org/10.1016/j.sna.2024.115522

[23] D. He *et al.*, "Secure rfid authentication schemes," *IEEE Communications Surveys & Tutorials*, 2017. https://doi.org/10.1109/COMST.2016.2638709

[24] J. Choi *et al.*, "Rfid-enabled automatic entry systems for smart campuses," *IEEE Access*, 2022. https://doi.org/10.1109/ACCESS.2022.3145672